Supporting information

Electric field mediated fibronectin-hydroxyapatite interaction: A molecular insight

Subhadip Basu[a], Biswajit Gorai[b], Bikramjit Basu[a,c,*], and Prabal K. Maiti[b,*]

[a]Materials Research Centre, Indian Institute of Science, Bangalore-560012, India

[b]Center for Condensed Matter Theory, Department of Physics, Indian Institute of Science, Bangalore-560012, India

[c]Center for Biosystems Science and Engineering, Indian Institute of Science, Bangalore-560012, India

* Joint corresponding authors; e-mail: bikram@iisc.c.in (B.Basu); maiti@iisc.ac.in (P.K. Maiti)

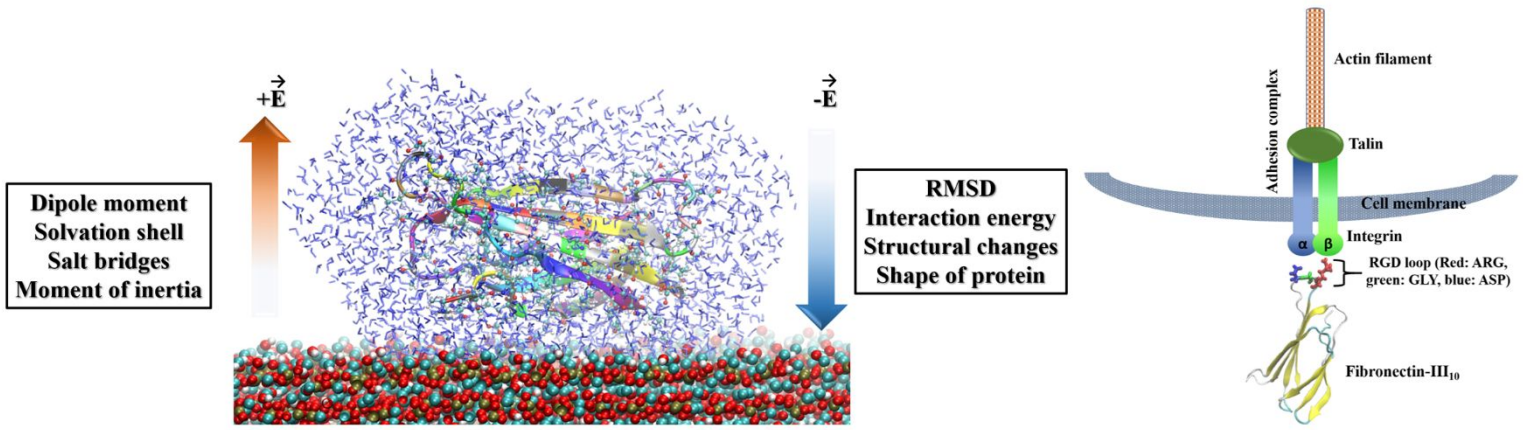

Fig. S1: Schematic representation of the simulation model used to understand the influence of the electric field on protein-material interaction. Some of the key aspects, quantitatively studied in this work, has been mentioned. Biological importance of RGD loop of FN in cell material interaction has also been pictorially depicted. Here, RMSD stands for root mean square deviation.

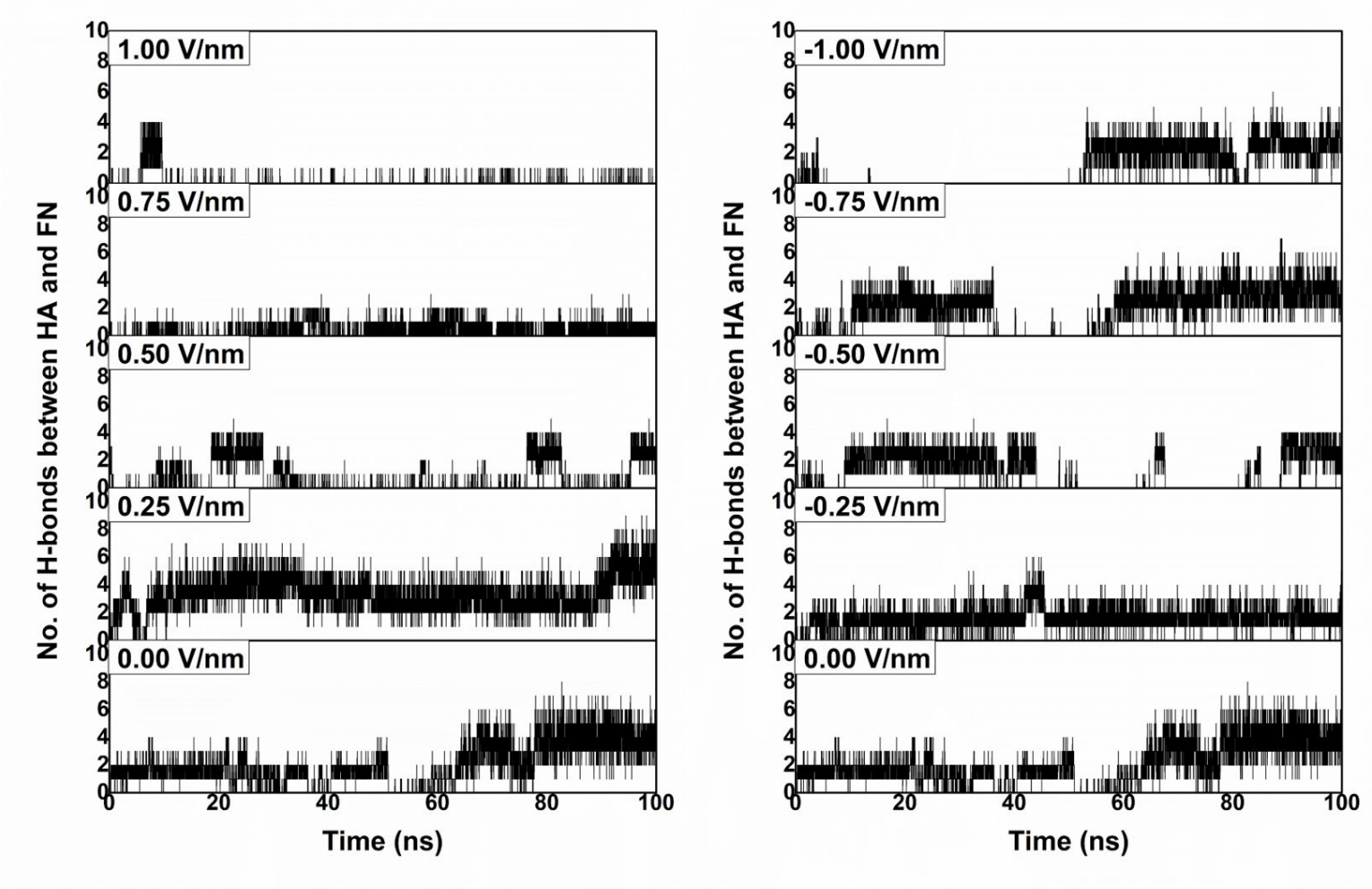

Fig. S2: Formation of hydrogen bonds is one of the principal means of protein-material interaction. Time-evolution of hydrogen bonds formed between fibronectin and HA at different field strengths.

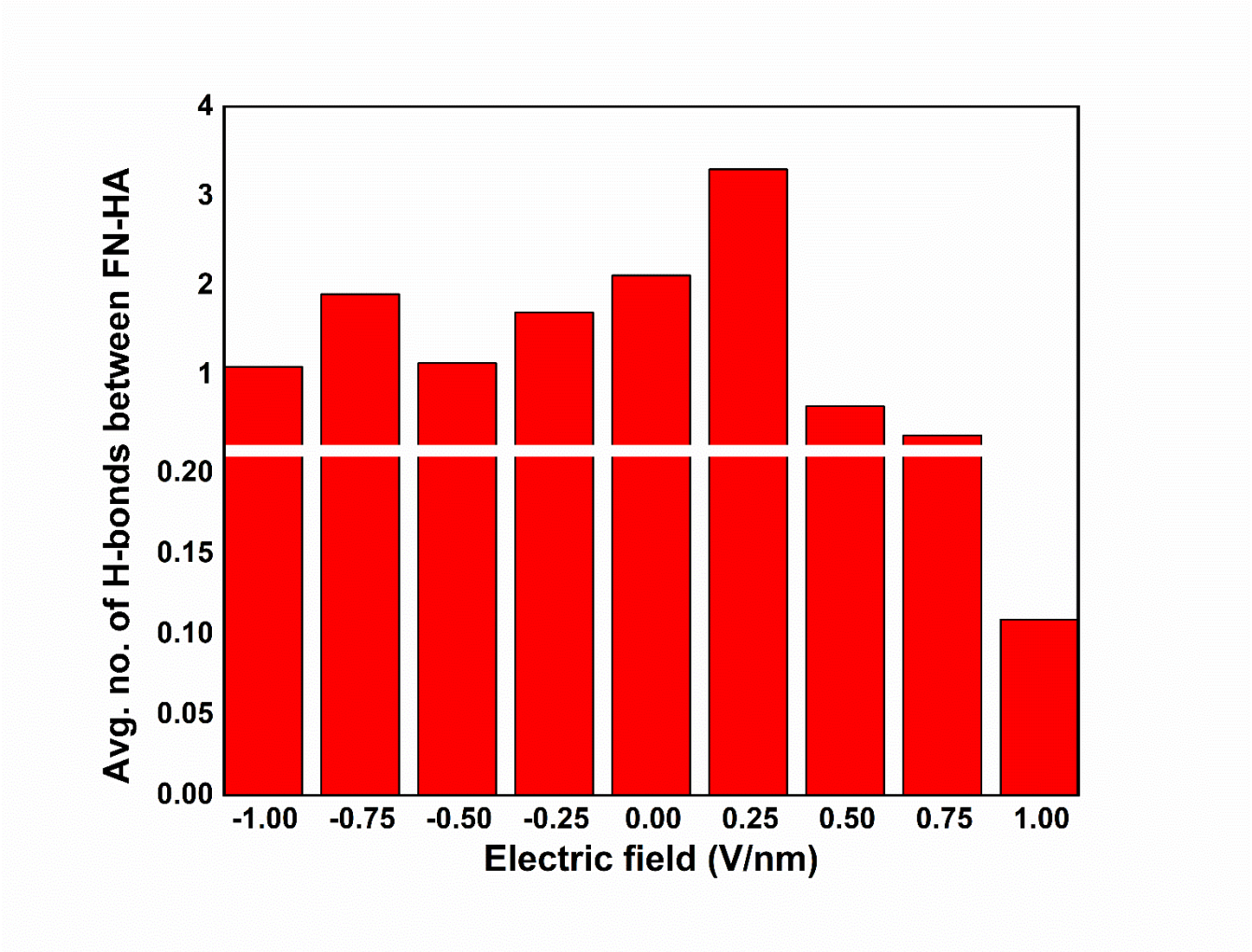

Fig. S3: Average number of hydrogen bonds formed between HA and FN at different electric fields.

S1. Hydrogen bond formation between FN and HA

Fig. S2 represents external field dependent time evolution of number of hydrogen bonds formed between HA and FN. The maximum number of hydrogen bonds was observed at field strength of 0.25 V/nm and these were reduced at higher field strength. The number of H-bonds was recorded to be comparatively higher at negative field values (Fig. S2). The decrease in the average number of hydrogen bonds was noted with an increase in the field strength, applied in an anti-parallel manner (Fig.S3). A slight increase was recorded at field strength of -0.75 V/nm (Fig. S3).

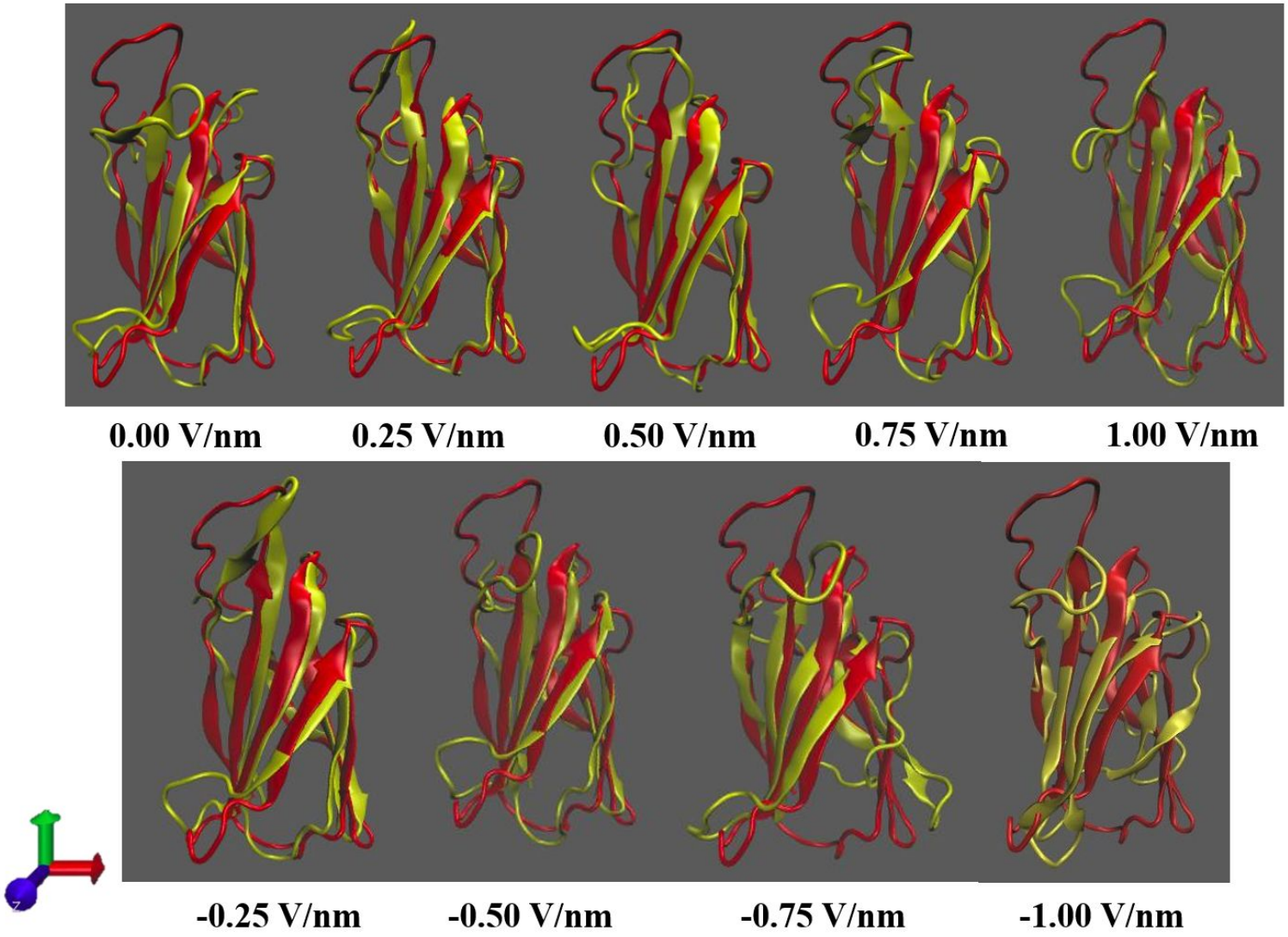

Fig. S4: Electric field application can influence protein conformation. Comparison of initial and final structure of fibronectin (colour code: Red: initial structure; yellow: final structure after 100 ns simulation. Axis colour code: Red: x, green: y, blue: z). Note that, conformational changes take place majorly in loop areas.

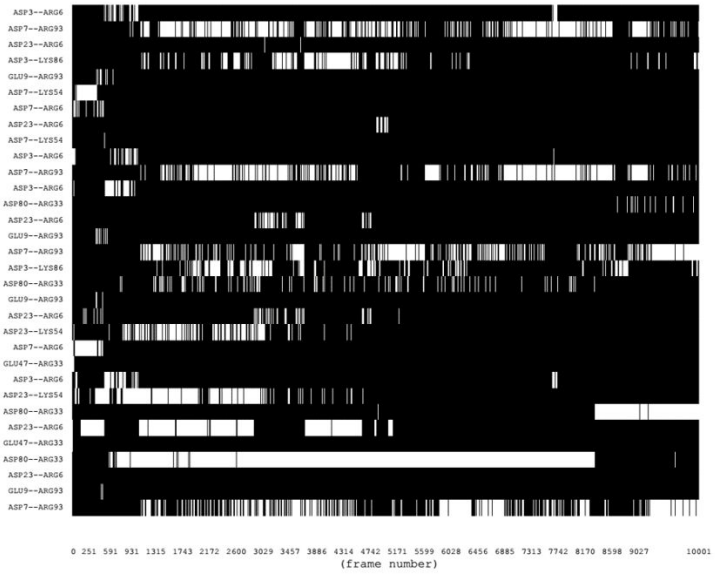

-1.00 V/nm

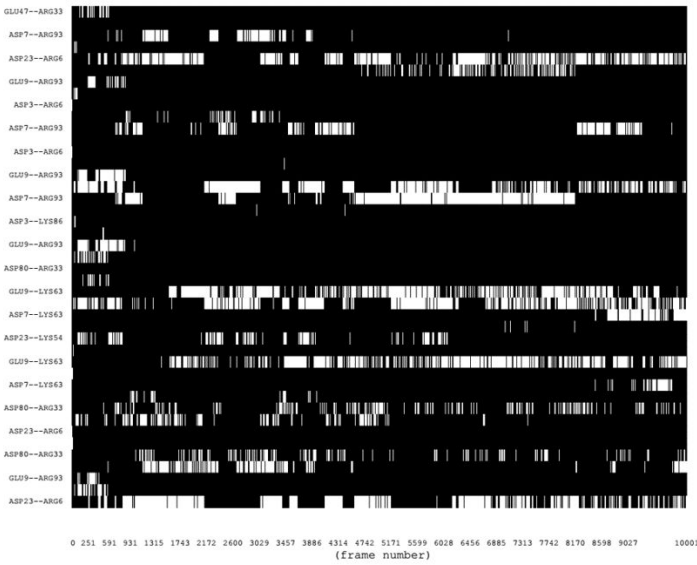

-0.75 V/nm

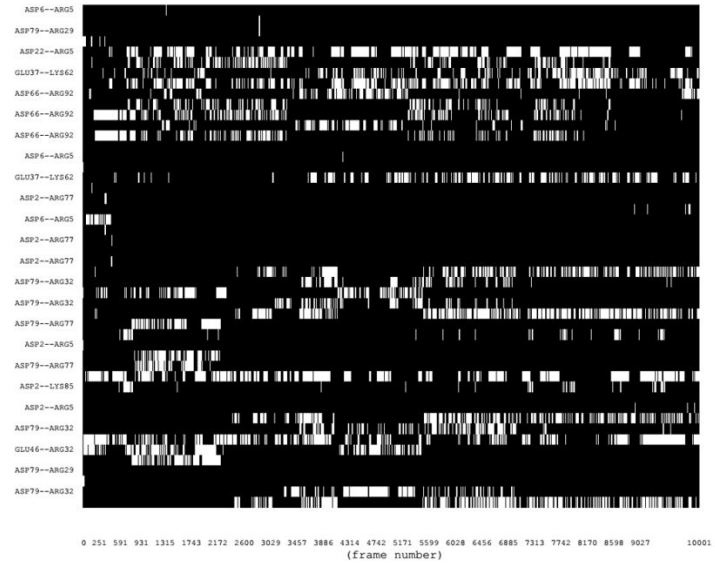

-0.50 V/nm

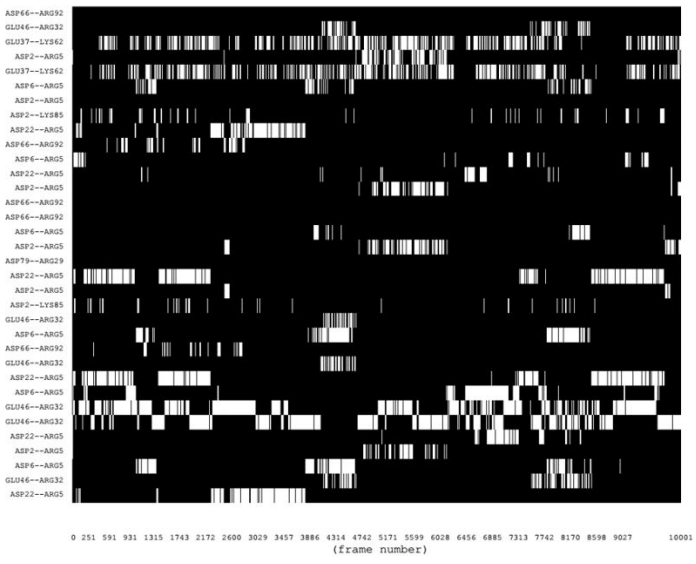

-0.25 V/nm

(a)

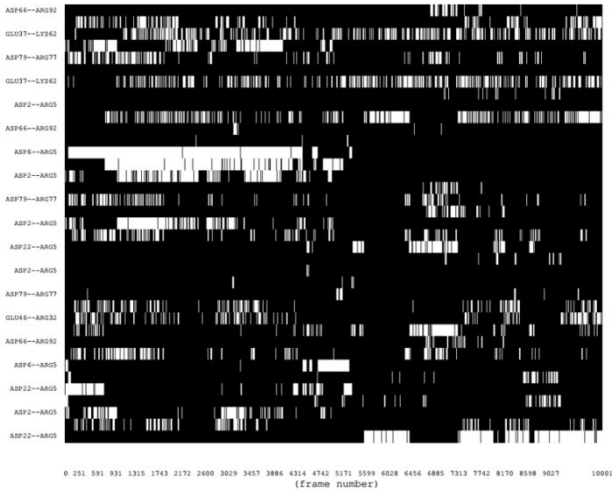

(b) **0.00 V/nm**

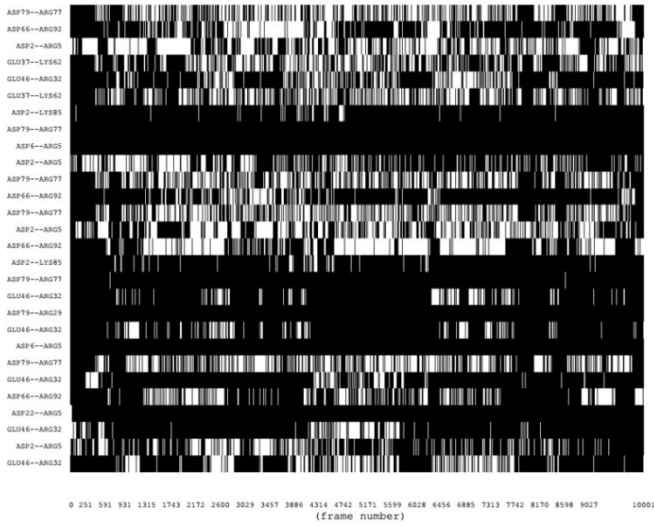

0.25 V/nm

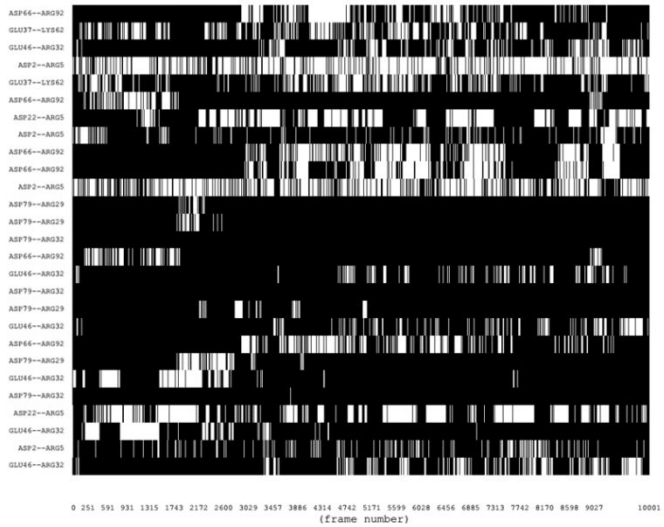

0.50 V/nm

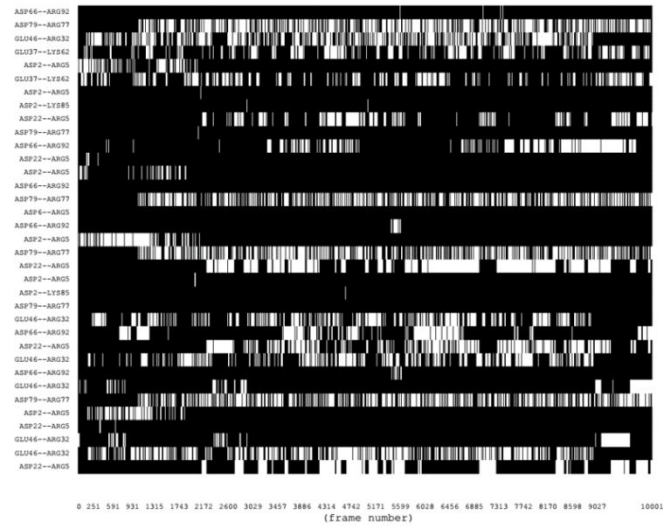

0.75 V/nm

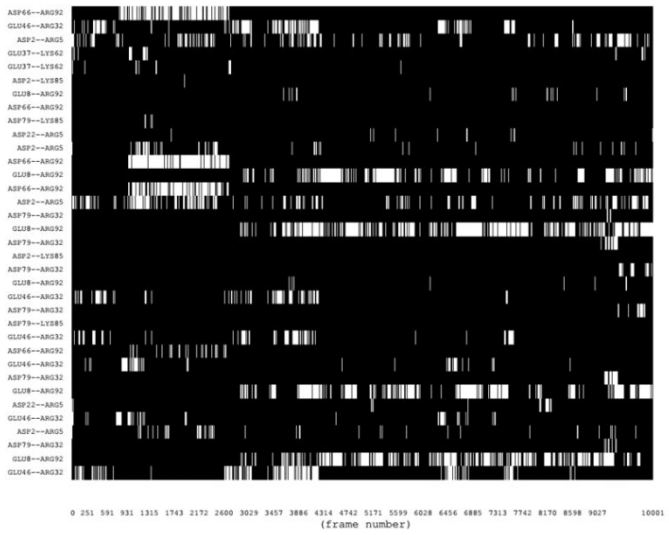

1.00 V/nm

(c)

Fig. S5: Temporal evolution of salt bridge networks of FN at (a) negative (b) zero and (c) positive electric fields. (colour Code: Black: no salt bridge, white: salt bridge present)

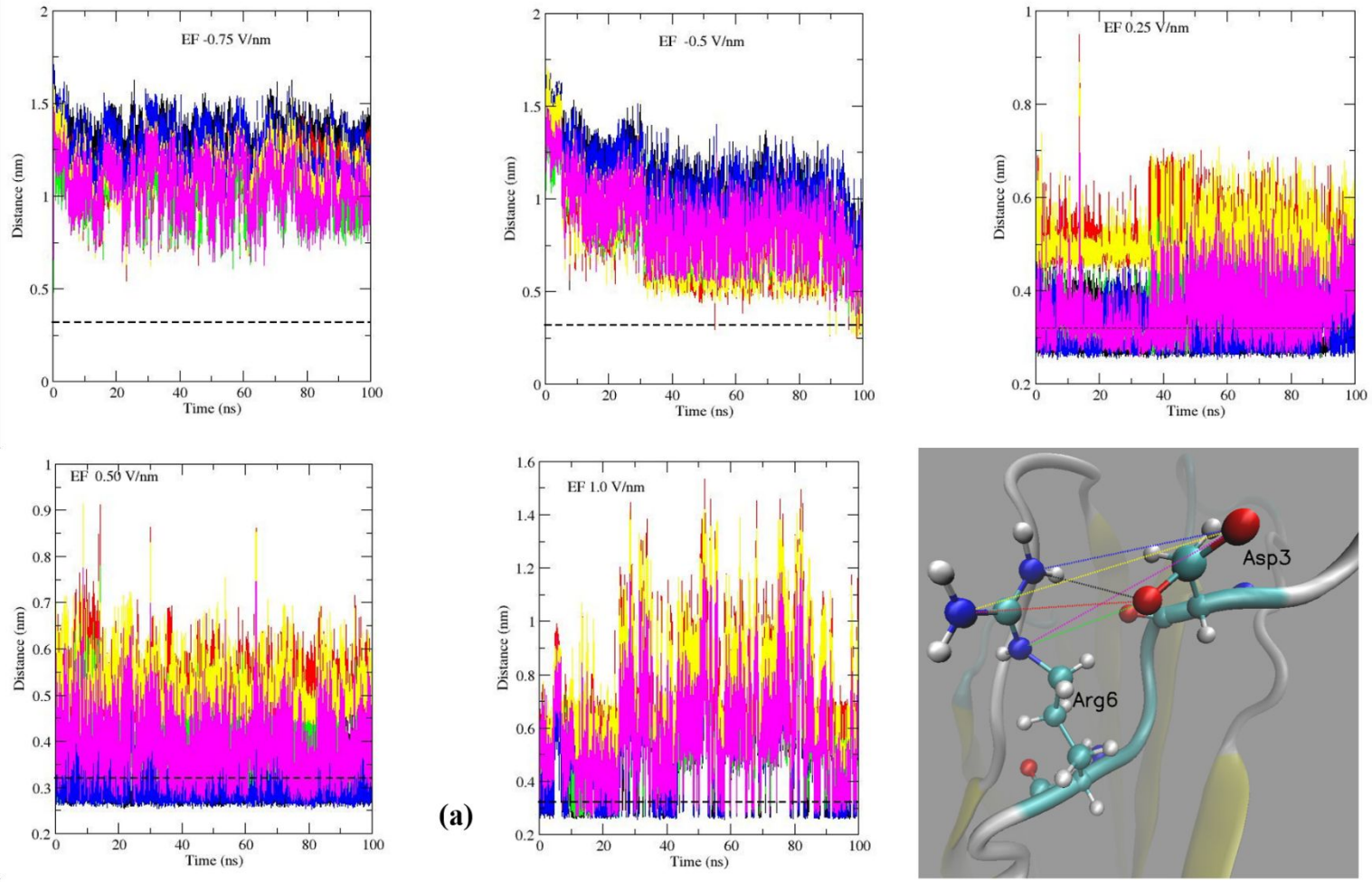
EF -0.75 V/nm
EF -0.5 V/nm
EF 0.25 V/nm
EF 0.50 V/nm
EF 1.0 V/nm
Distance (nm)
Time (ns)
Asp3
Arg6

(a)

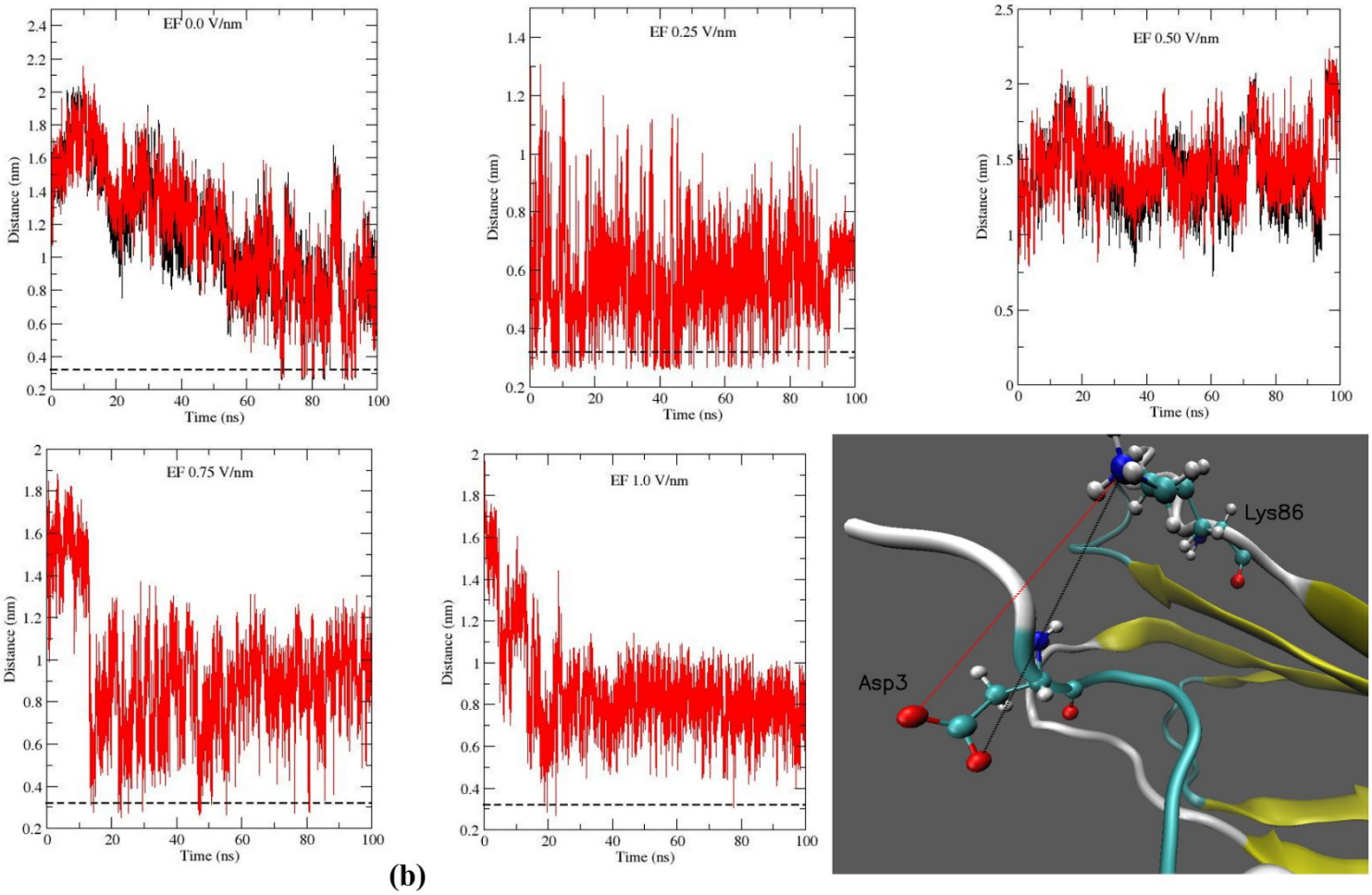
EF 0.0 V/nm
EF 0.25 V/nm
EF 0.50 V/nm
EF 0.75 V/nm
EF 1.0 V/nm
Distance (nm)
Time (ns)
Lys86
Asp3

(b)

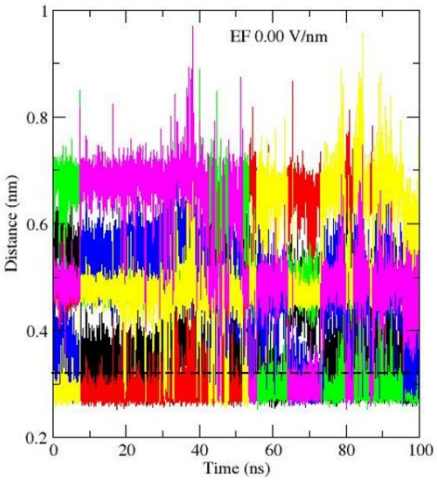
EF 0.00 V/nm
Distance (nm)
Time (ns)

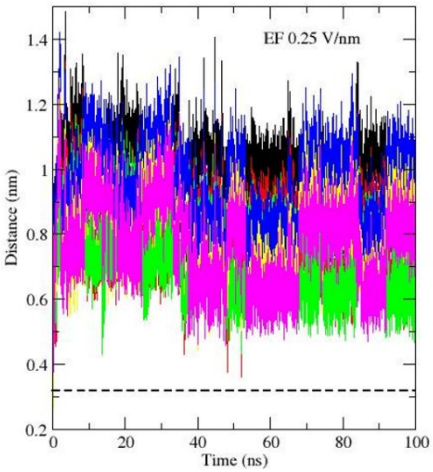
EF 0.25 V/nm
Distance (nm)
Time (ns)

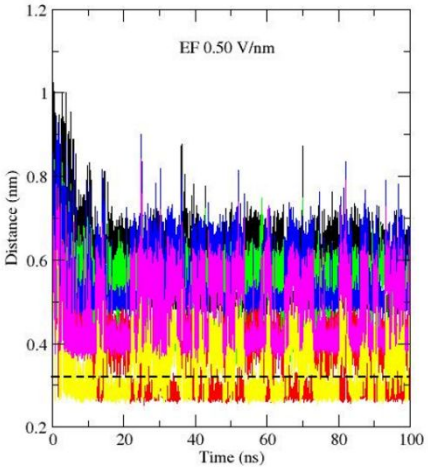
EF 0.50 V/nm
Distance (nm)
Time (ns)

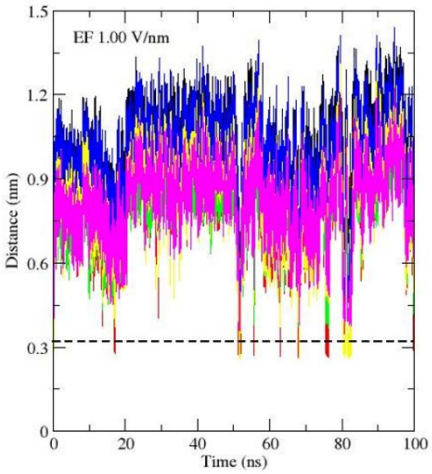
EF 1.00 V/nm
Distance (nm)
Time (ns)

(c)

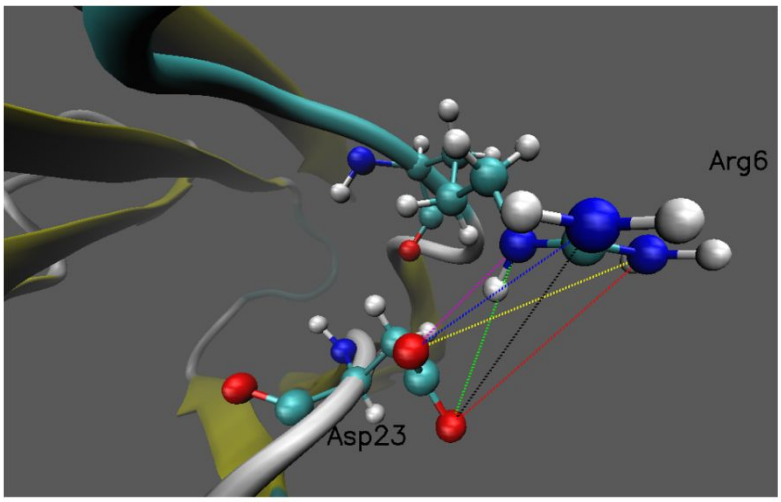
Arg6
Asp23

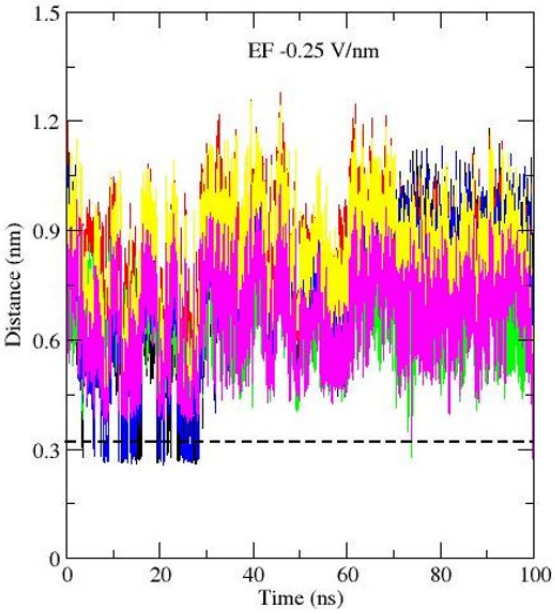
EF -0.25 V/nm
Distance (nm)
Time (ns)
0
0.3
0.6
0.9
1.2
1.5
0
20
40
60
80
100

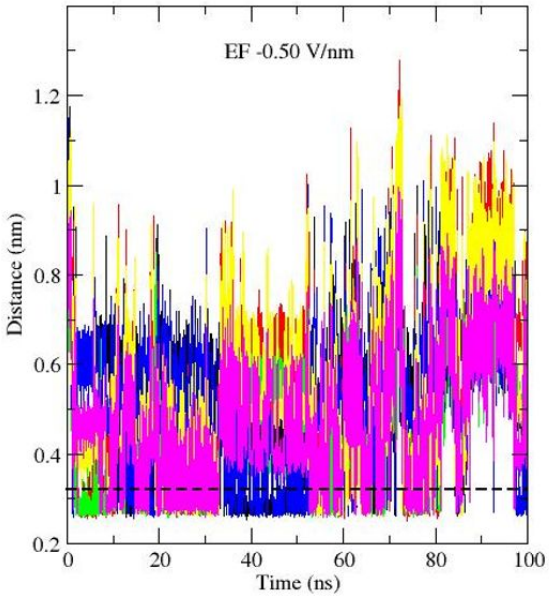
EF -0.50 V/nm
Distance (nm)
Time (ns)
0.2
0.4
0.6
0.8
1
1.2
0
20
40
60
80
100

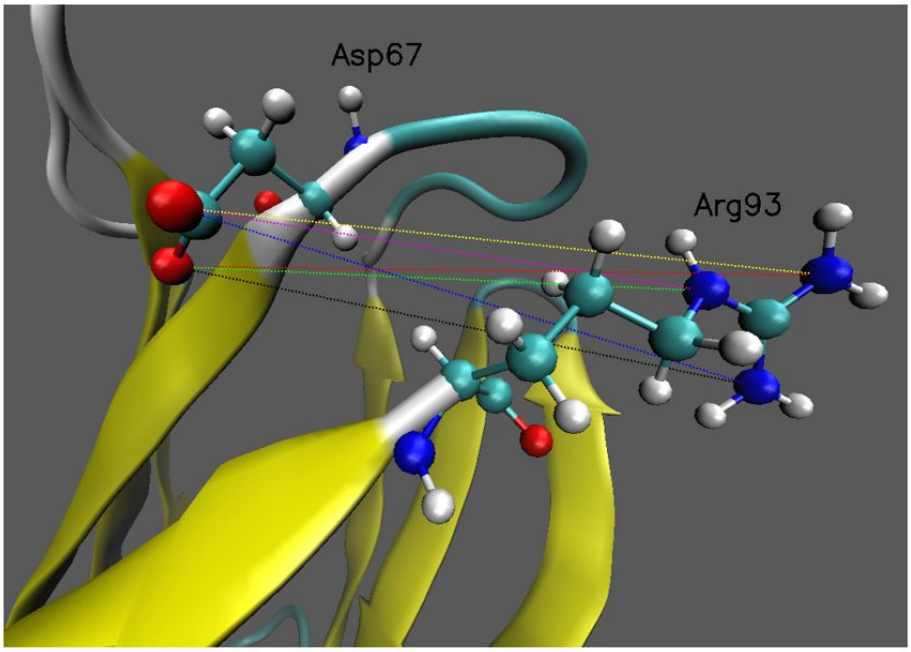
Asp67
Arg93

(d)

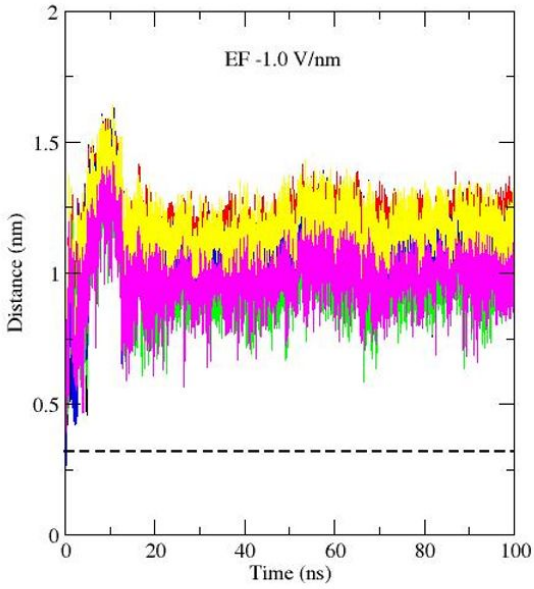

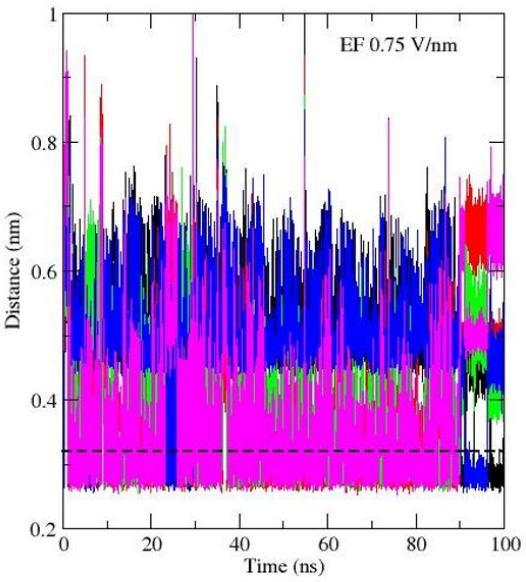

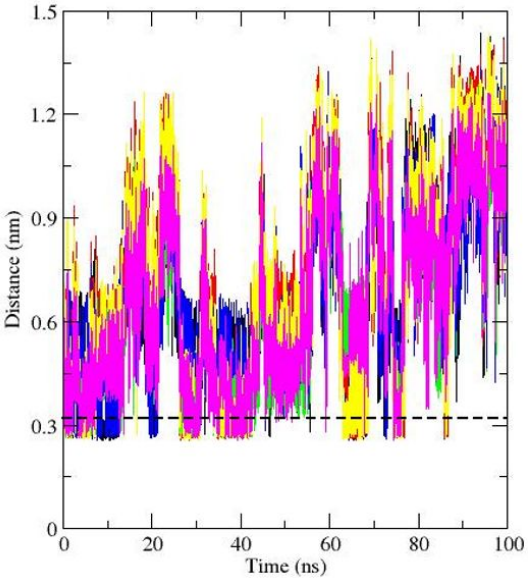

(e)

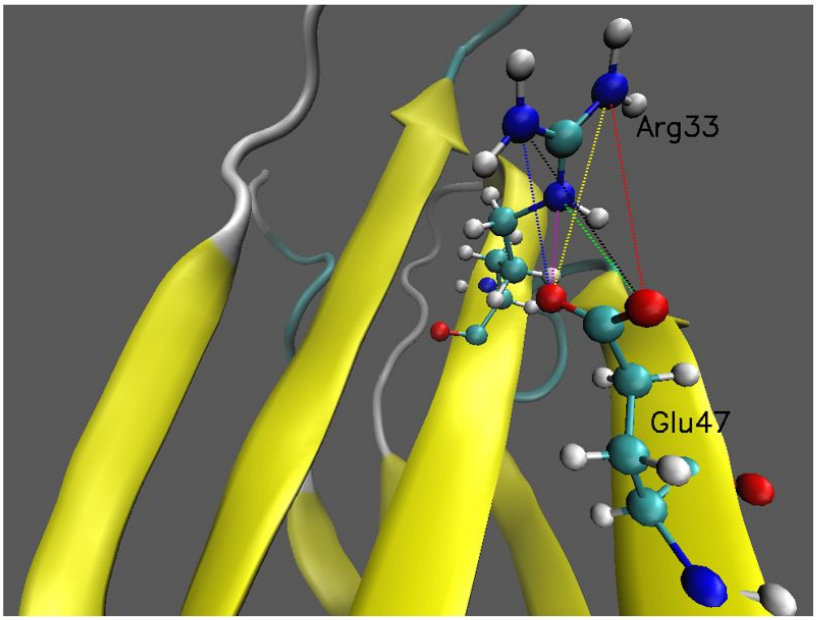

Fig. S6: Different salt bridges are switching on and off in the course of simulation. Distance between different O and N atomic pairs of (a) Asp3-Arg6 (b) Asp3-Lys86 (c) Asp23-Arg6 (d) Asp67-Arg93 and (e) Glu47-Arg33 salt bridge forming residues. Identical colours have been used to present the distances between different O-N atomic pairs in the plots and in the associated cartoons. Atomic colour code: Red: O, blue: N, cyan: C, white: H. The dashed horizontal line represents the cut off distance (0.32 nm) of salt bridge formation.

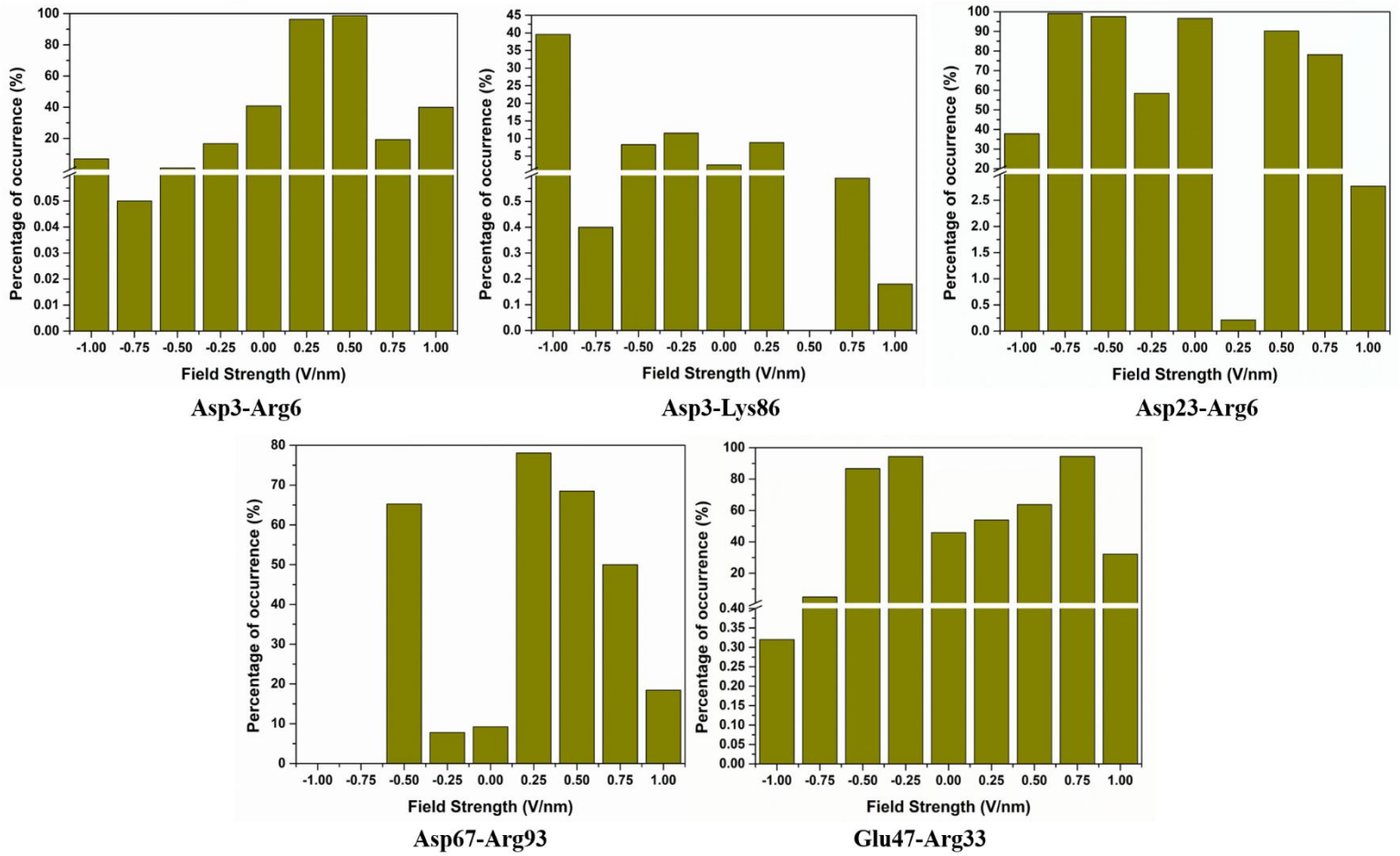

Fig. S7: Salt bridges play important role in stabilizing protein structure. Percentage of occurrence of different salt bridges at various electric field strength.

S2. Temporal evolution of salt bridges

The temporal evolution of different salt bridges has been presented in Fig. S5 in the supplementary section. A general observation is that the stability of the salt bridges was affected at high field strength (Fig. S5) In order to obtain a quantitative aspect, the percentage of occurrence (occurrence frequency) of some selected salt bridge nets were calculated and presented graphically in Fig.S7. From Fig. S7, it can be easily seen that different salt bridges responded differently under the influence of external field. The underlying reason is the non-identical behaviour of O-N atomic distances in different salt bridge forming residue pairs under the influence of same electric field intensity (Fig. S6). However, the occurrence frequency was found to be low at high field intensity in most of the cases, in corroboration with the information provided in Fig. S5 in supplementary section (Fig. S7). From this observation, it can be easily concluded that, the overall stability of the FN structure hindered at high field strength.

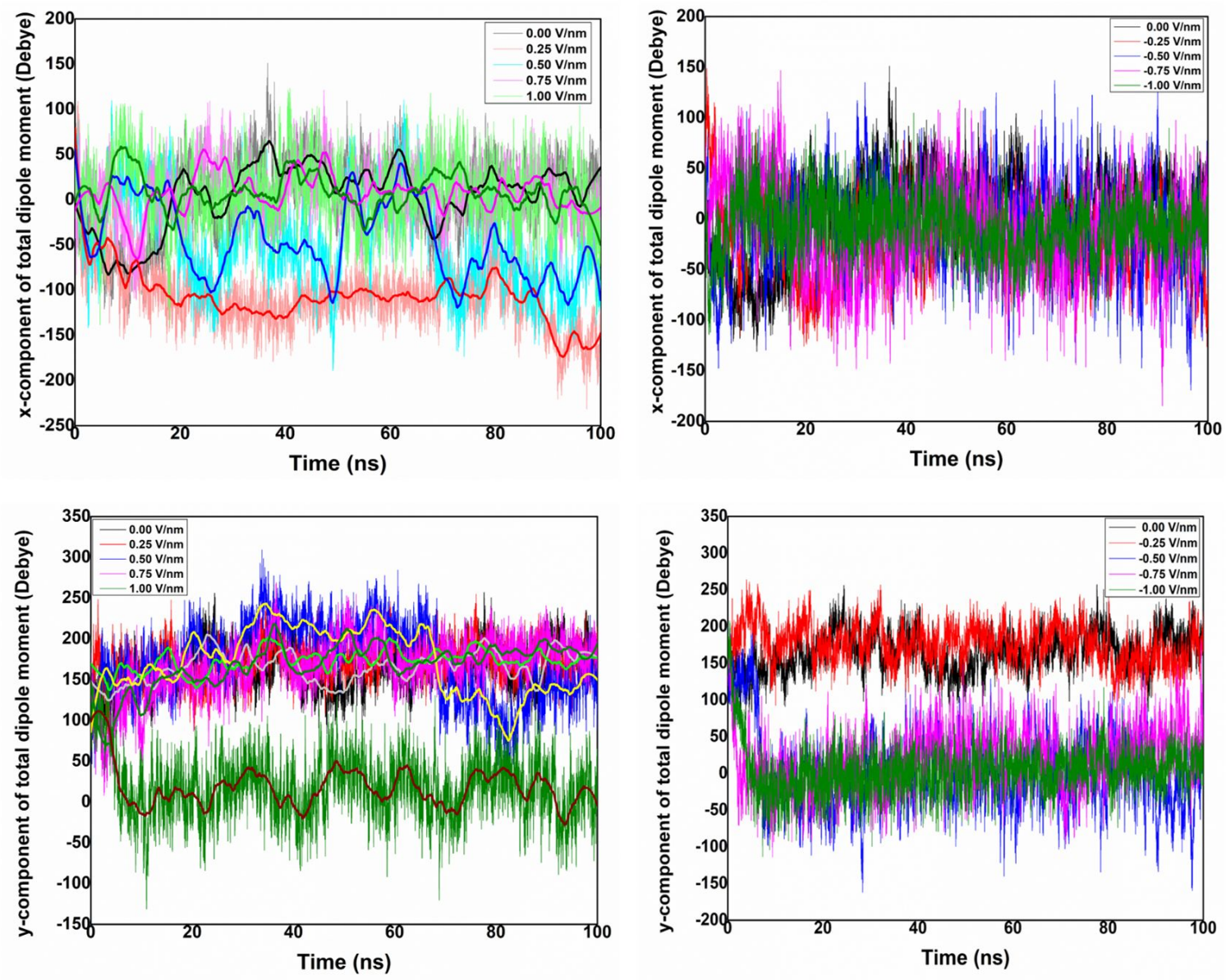

Fig. S8: x and y component of dipole moment of FN at different electric fields.

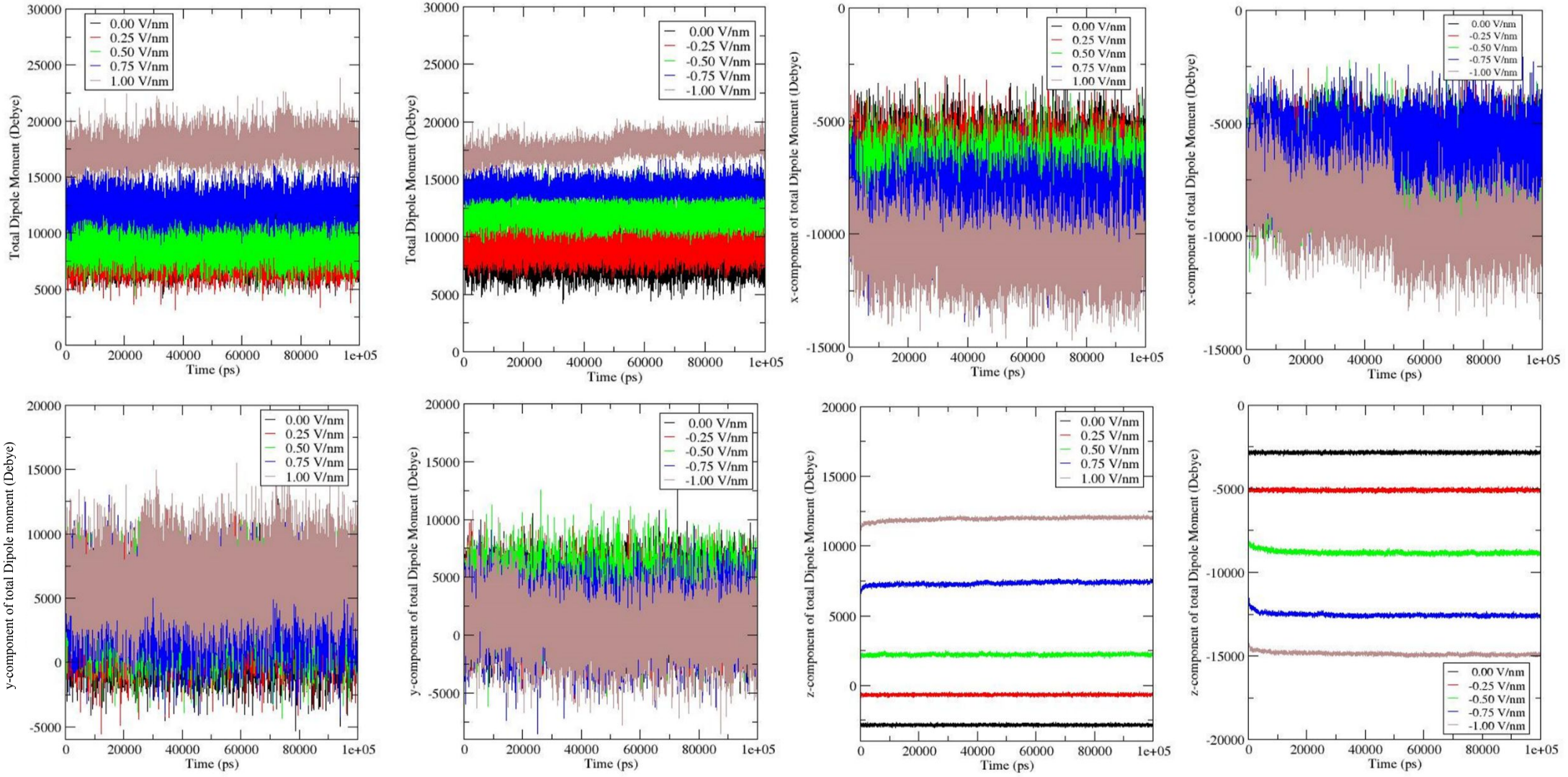

Fig. S9: Total, x, y and z component of dipole moment of HA at different electric fields.

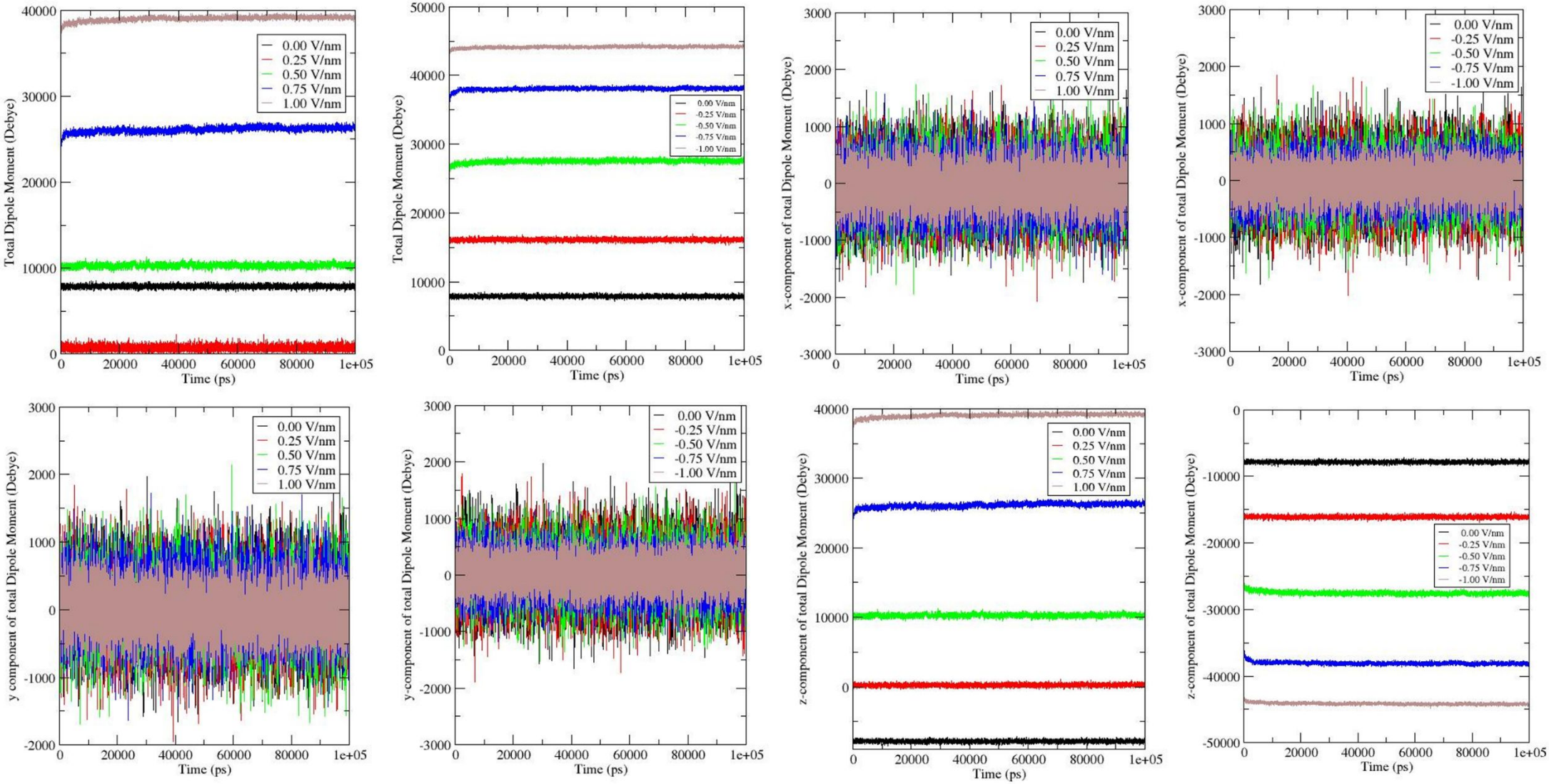

Fig. S10: Electric field dependency of total, x, y and z component of dipole moment of water.

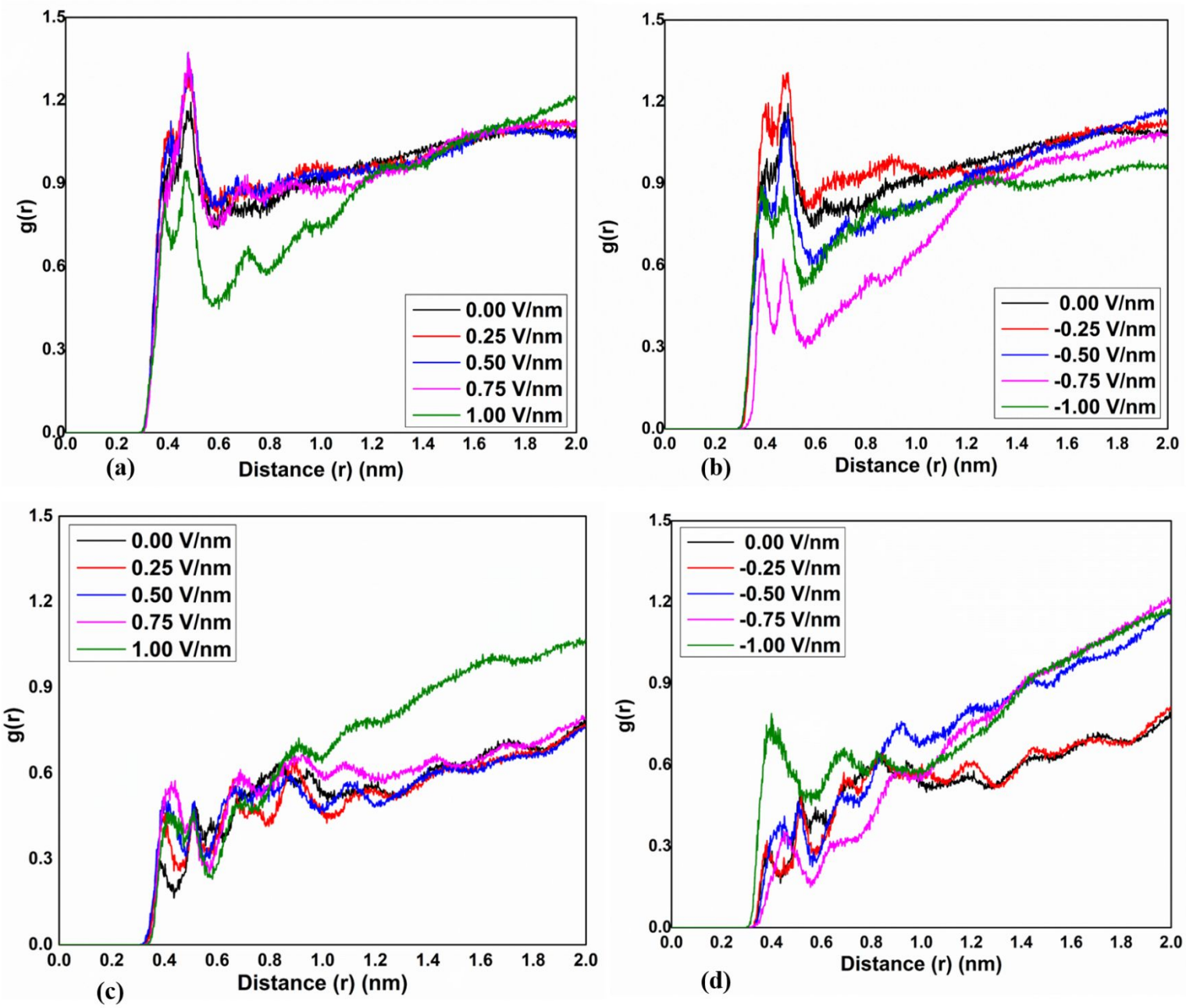

Fig. S11: Solvation shell around the protein plays an important role in adsorption. Radial distribution function (RDF; $g_{OC}(r)$) of water oxygen atoms surrounding C_α atom of a (a)-b) hydrophilic (Ser53) and (c)-(d) hydrophobic (Leu8) residue.

S3. Solvation shell around FN

As mentioned in the main article, the noticeable changes in the RDF peak intensity appeared only at high field strengths (Fig. S11). This indicates that, the presence of the electric field changed the solvation shell structure around the FN module, though not significantly.

There is a clear distinction between the arrangement of water molecules around the hydrophobic and hydrophilic residue (Fig. S11). The hydrophobic residues are usually buried into the inner surface of the protein and remains in limited contact with the solvent molecules.[1] On the other hand, the hydrophilic residues are exposed and are in direct contact with the water molecules.[1] This positional difference of the two types of residues results in the different orientation of water molecules surrounding them, which eventually leads to significantly different RDF. The intensity of the peaks decreased at high positive field strengths positive for hydrophilic residue probably, because of the structural rearrangement of FN (Fig. S11(a)-(b)). The structural rearrangement results in less accessibility of Ser53 for solvent molecules. Hence, the peak intensity decreased. A significant change in RDF of hydrophobic residue can be noticed at -1.00 V/nm (Fig. S11(d)). This observation can be corroborated with the high RMSD of FN at -1.00 V/nm (Fig. 6). At high field strength, the protein structure was found to be in its most altered condition and even the β-strands were affected (Fig. 6). Due to this conformal change, the inner part of FN got exposed to the solvent and the height RDF peak increased.

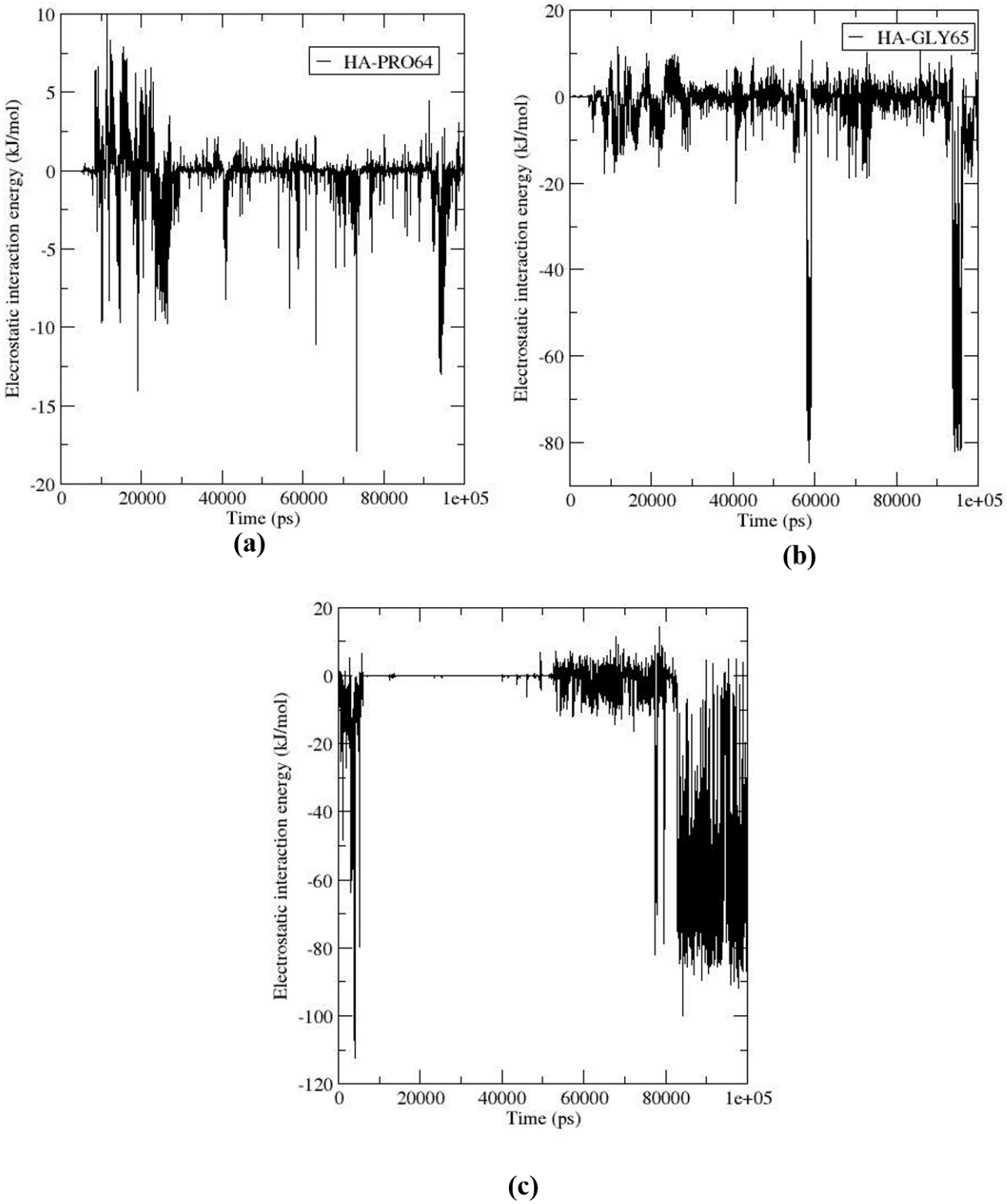

Fig. S12: Neutral residues interact weakly with HA surface, as evident from interaction energy of neutral residues close to surface at (a)-(b) 1.00 V/nm and (c) -1.00 V/nm.

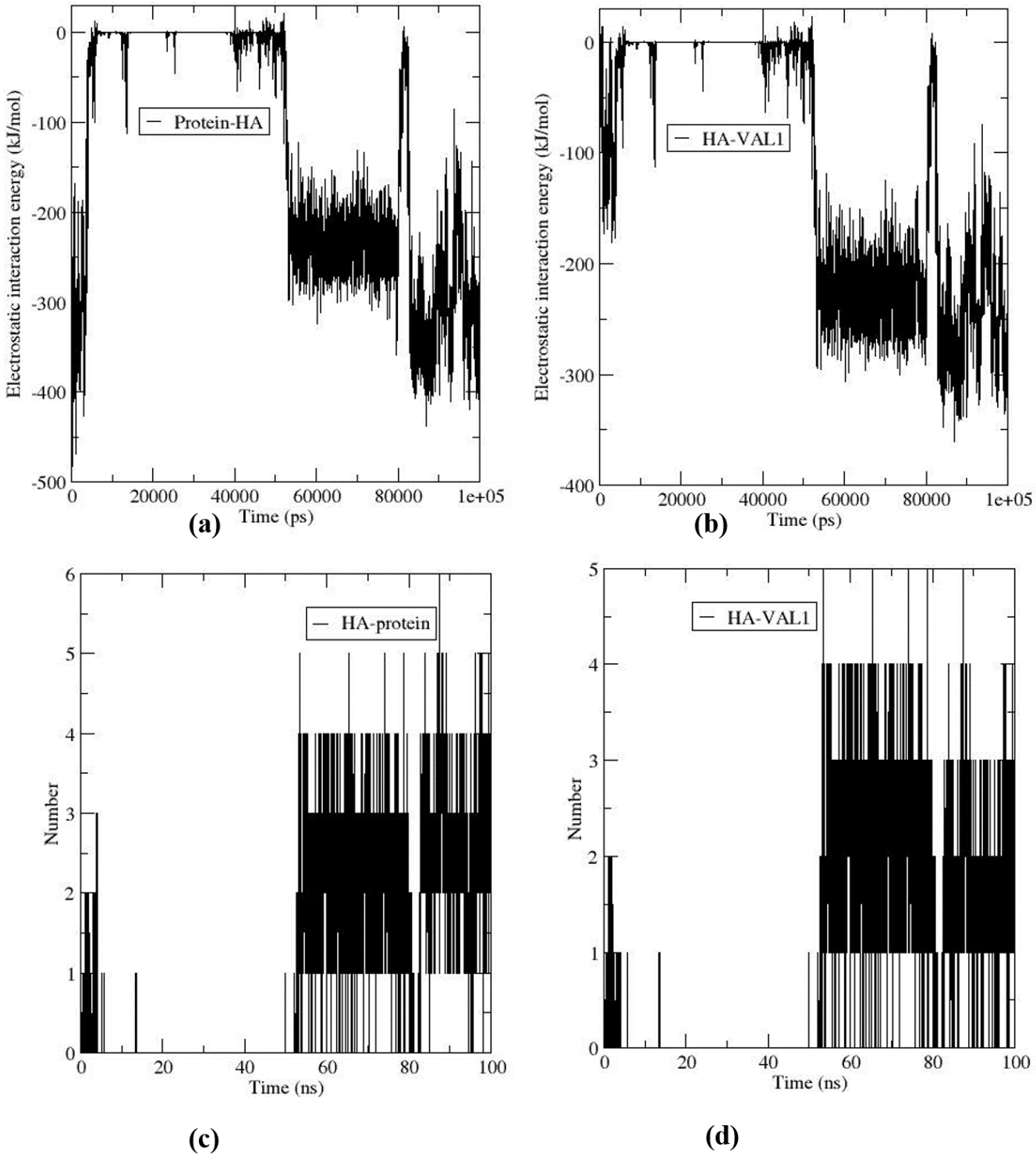

Fig. S13: Comparison of (a)-(b) interaction energy and (c)-(d) number of hydrogen bonds between protein-HA and VAL1-HA at electric field strength of -1.00 V/nm.

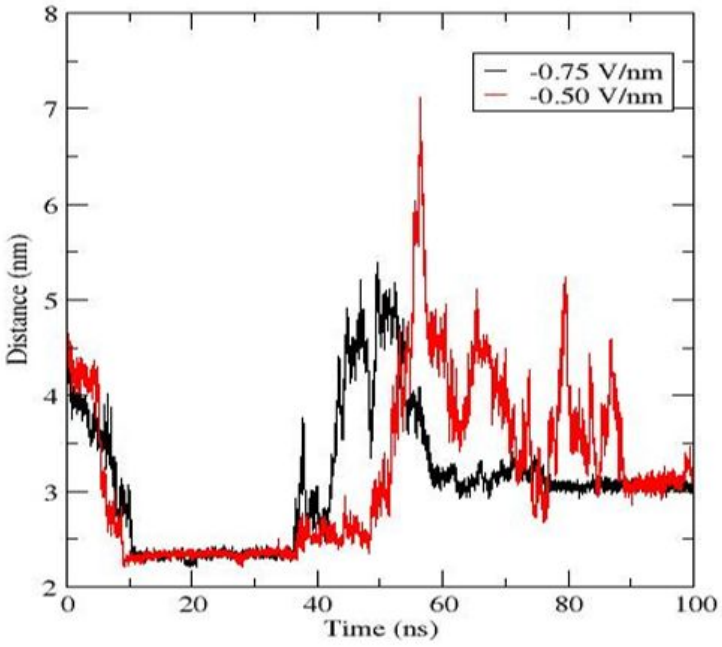

(a)

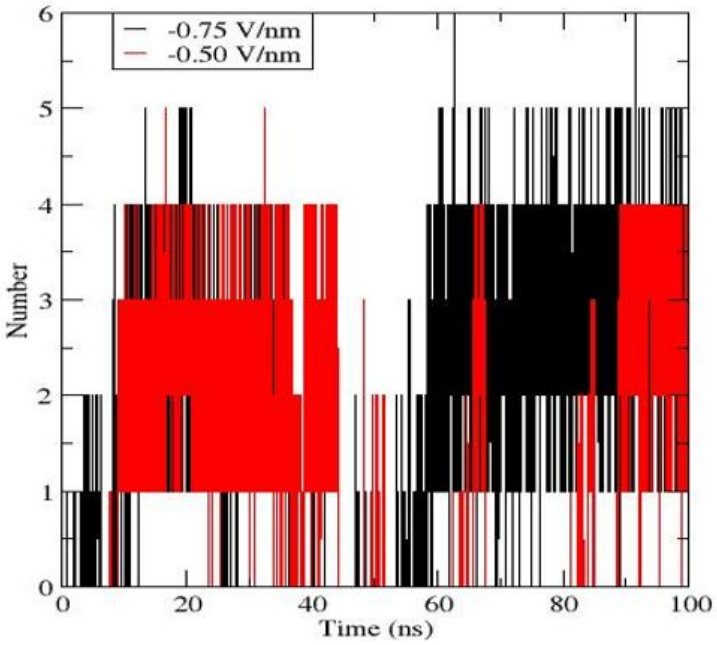

(b)

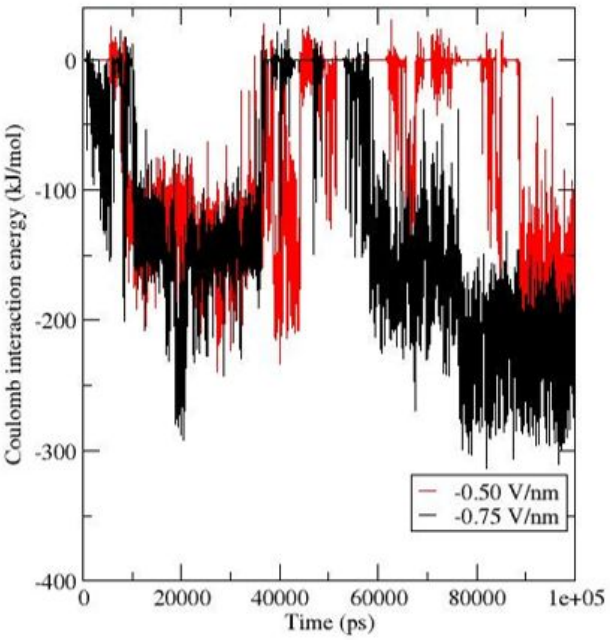

(c)

Fig. S14: (a) COM-COM distance (b) number of hydrogen bonds and (c) electrostatic interaction energy between Arg78 and HA at different time points.

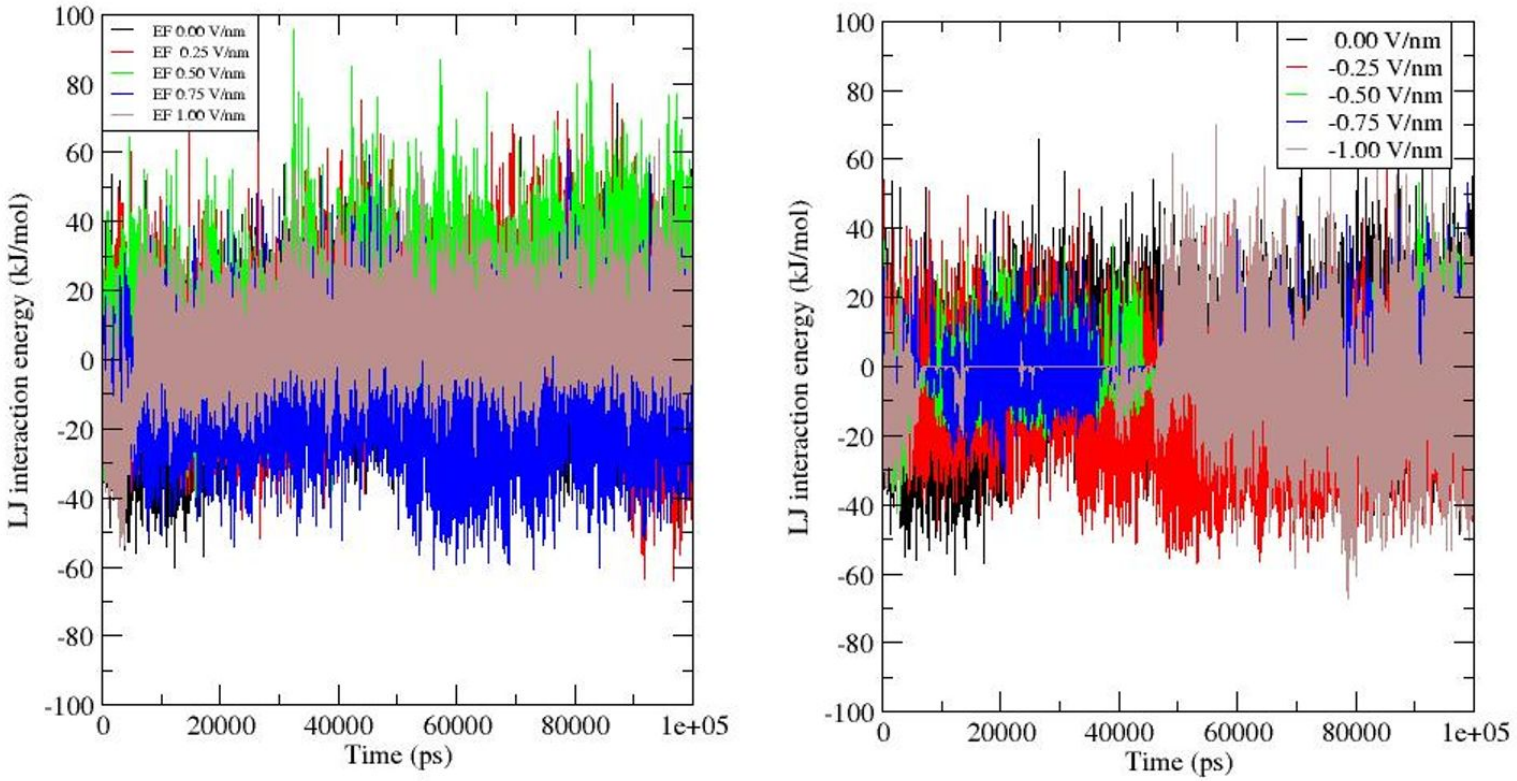

Fig. S15: Non-bonded interaction energy between HA and FN at different electric fields.

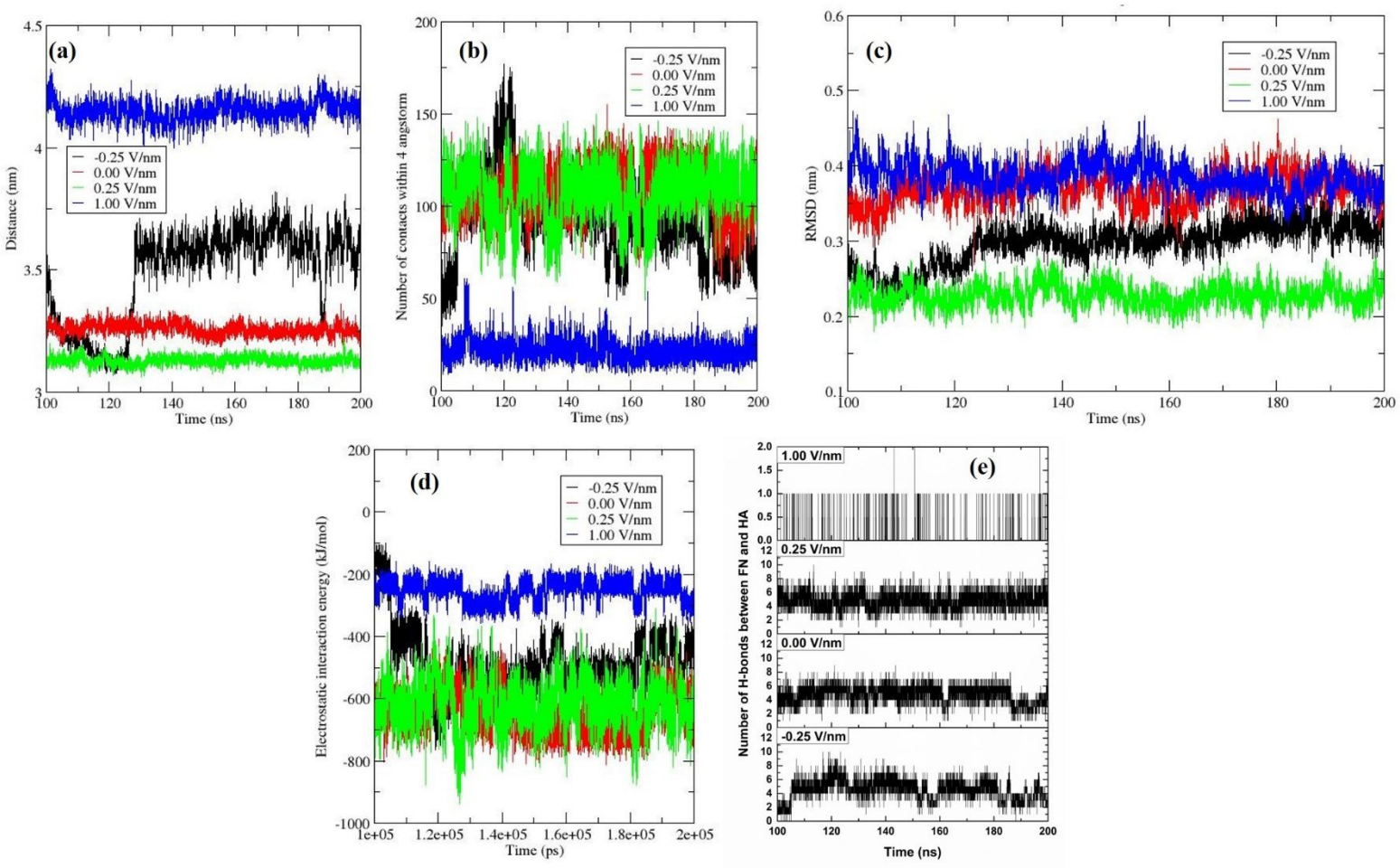

Fig. S16: Long –term behaviour of FN-HA system under external electric field. Temporal evolution of (a) COM-COM distance of FN-HA, (b) number of contacts between FN and HA, (c) RMSD of FN backbone, (d) electrostatic interaction energy between FN and HA, and (e) number of hydrogen bonds between HA and FN.

S4: Long-term adsorption behaviour of FN on HA

Fig. S16 represents results obtained from additional 100ns simulation of FN-HA system under the influence of electric field. From Fig. S16, it is evident that, the adsorption is not favoured in presence of high field strength (1.00 V/nm). The FN module remained adsorbed strongly on the HA surface up to 0.25 V/nm of field strength. Throughout the simulation window, the FN maintained a steady distance from the surface (Fig. S16(a)) and interact with the surface via coulombic interaction and formation of the hydrogen bonds (Fig. S16 (d) and (e)). On the other hand, at 1.00 V/nm, the process of the formation of hydrogen bonds between HA and FN hindered (Fig. S16 (e)).In case of -0.25 V/nm, although FN remained adsorbed on the surface,

it could not maintain a steady distance from the surface (Fig. S16 (a)). Rather, it made a transition from strongly adsorbed state to a relatively weak adsorbed state (Fig. S16(a) and (d)). The time evolution of the number of contacts also supports the fact that, the adsorption is not favoured at high field strength (Fig. S16 (b)). The structure of the FN module has not changed significantly during the simulation timespan, as seen in Fig. S16 (c).

References

(1) Mehrnejad, F.; Ghahremanpour, M. M.; Khadem-Maaref, M.; Doustdar, F. Effects of Osmolytes on the Helical Conformation of Model Peptide: Molecular Dynamics Simulation. *J. Chem. Phys.* **2011**, *134* (3), 01B620.